Arthritis & Rheumatology
Vol. 75, No. 5, May 2023, pp 794–805
DOI 10.1002/art.42413

American College of Rheumatology
Empowering Rheumatology Professionals

Amplification of Inflammation by Lubricin Deficiency Implicated in Incident, Erosive Gout Independent of Hyperuricemia

Khaled Elsaid,[1] Tony R. Merriman,[2] Leigh-Ana Rossitto,[3] Ru Liu-Bryan,[4] Jacob Karsh,[5] Amanda Phipps-Green,[6] Gregory D. Jay,[7] Sandy Elsayed,[1] Marwa Qadri,[8] Marin Miner,[9] Murray Cadzow,[6] Talia J. Dambruoso,[10] Tannin A. Schmidt,[11] Nicola Dalbeth,[12] Ashika Chhana,[12] Jennifer Höglund,[13] Majid Ghassemian,[14] Anaamika Campeau,[3] Nancy Maltez,[5] Niclas G. Karlsson,[15] David J. Gonzalez,[16] and Robert Terkeltaub[17]

Objective. In gout, hyperuricemia promotes urate crystal deposition, which stimulates the NLRP3 inflammasome and interleukin-1β (IL-1β)–mediated arthritis. Incident gout without background hyperuricemia is rarely reported. To identify hyperuricemia-independent mechanisms driving gout incidence and progression, we characterized erosive urate crystalline inflammatory arthritis in a young female patient with normouricemia diagnosed as having sufficient and weighted classification criteria for gout according to the American College of Rheumatology (ACR)/EULAR gout classification criteria (the proband).

Methods. We conducted whole-genome sequencing, quantitative proteomics, whole-blood RNA-sequencing analysis using serum samples from the proband. We used a mouse model of IL-1β–induced knee synovitis to characterize proband candidate genes, biomarkers, and pathogenic mechanisms of gout.

Results. Lubricin level was attenuated in human proband serum and associated with elevated acute-phase reactants and inflammatory whole-blood transcripts and transcriptional pathways. The proband had predicted damaging gene variants of *NLRP3* and of inter-α trypsin inhibitor heavy chain 3, an inhibitor of lubricin-degrading cathepsin G. Changes in the proband's serum protein interactome network supported enhanced lubricin degradation, with cathepsin G activity increased relative to its inhibitors, SERPINB6 and thrombospondin 1. Activation of Toll-like receptor 2 (TLR-2) suppressed levels of lubricin mRNA and lubricin release in cultured human synovial fibroblasts ($P < 0.01$). Lubricin blunted urate crystal precipitation and IL-1β induction of xanthine oxidase and urate in cultured macrophages ($P < 0.001$). In lubricin-deficient mice, injection of IL-1β in knees increased xanthine oxidase–positive synovial resident M1 macrophages ($P < 0.05$).

Conclusion. Our findings linked normouricemic erosive gout to attenuated lubricin, with impaired control of cathepsin G activity, compounded by deleterious *NLRP3* variants. Lubricin suppressed monosodium urate crystallization and blunted IL-1β–induced increases in xanthine oxidase and urate in macrophages. The collective activities of articular lubricin that could limit incident and erosive gouty arthritis independently of hyperuricemia are subject to disruption by inflammation, activated cathepsin G, and synovial fibroblast TLR-2 signaling.

INTRODUCTION

In gout, hyperuricemia drives tissue supersaturation with urate, with consequent deposition of monosodium urate crystals in tophi on the articular cartilage surface and in other joint tissues (1). Within tophi, urate crystal aggregates are mixed with foci of chronic synovitis, granulomatous and multicellular pannus-like inflammation, and fibrosis (2). Urate crystal ingestion by

Dr. Elsaid's work was supported by NIH grant AR-067748. Dr. Merriman's work was supported by NIH grant AR-075990 and Health Research Council of New Zealand award 14-527. Dr. Rossitto's work was supported by NIH grant T32-GM-007752. Dr. Liu-Bryan's work was supported by VA Research Service award I01-BX-002234 and a Rheumatology Research Foundation Innovation Research Award. Dr. Jay's work was supported by NIH grant AR-067748. Dr. Dalbeth's work was supported by Health Research Council of New Zealand award 19-232. Dr. Chhana's work was supported by a Royal Society of New Zealand Rutherford Foundation Post-Doctoral Research Fellowship. Dr. Campeau's work was supported by NIH grant T32-AR-064194. Dr. Karlsson's work was supported by the Swedish state under an agreement between the Swedish government and the county council, the Agreement for Medical Education and Research (ALF) grant ALFGBG-722391, Swedish Research Council grant 621-2013-5895, Petrus and Augusta Hedlunds Foundation grant M-2016-0353, and AFA insurance research fund grant dnr-150150. Dr. Gonzalez's work was supported by the University of California,

monocytes and macrophages stimulates NLRP3 inflammasome activation and release of interleukin-1β (IL-1β) (1,3). The consequent endothelial and phagocyte activation amplifies inflammatory arthritis (1,3) and promotes NETosis, which can augment tissue urate levels (4) and modulate urate crystal aggregation, tophus development, and chronicity of gouty arthritis (5).

The major effects of gene variants on urate transport, purine metabolism, and serum urate predisposing to hyperuricemia, gout, and tophaceous disease include population-specific loss of function polymorphisms of the ATP-binding cassette urate transporter ABCG2 (6). Disease duration, older age, and chronic kidney disease are among the other risk factors for tophi (7). However, genome-wide association studies (GWAS) on major gout have principally included hyperuricemia cases (8). Consequently, the genetic factors that promote progression of hyperuricemia to incident gout and development of tophaceous and erosive gout phenotypes are poorly understood (8). Notably, asymptomatic hyperuricemia is over 5 times as prevalent as gout (9). Furthermore, gouty urate levels in synovial fluid have been reported to be enriched relative to urate levels in serum (10). Hence, passive filtering of excess circulating urate into joints cannot be the sole factor stimulating articular urate crystal deposition (11). Moreover, signals for changes in urate levels identified by GWAS are enriched for genes expressed in joint tissues, including the synovium (12).

To identify novel gene variants and constitutively active mediators that might limit the development of gout in a minority of patients with hyperuricemia, as well as the gene variants and mediators that suppress disease progression, we performed a systematic analysis of serum from a proband, a young female patient who had normouricemia and met sufficient and weighted classification criteria for gout according to the 2015 American College of Rheumatology (ACR)/EULAR classification criteria (13) and who developed erosive arthritis. In serum samples from the proband, we identified attenuation of the proteoglycan 4 (*PRG4*) gene product lubricin, examined linked genetic variants, and investigated other changes particularly permissive for NLRP3/IL-1β–mediated autoinflammation, proteolysis of lubricin, and fibrosis.

PATIENTS AND METHODS

The data used for the analyses described in this article were obtained from https://gtexportal.org/home/.

The Supplementary Materials and Methods and Additional Results, available on the *Arthritis & Rheumatology* website at https://onlinelibrary.wiley.com/doi/10.1002/art.42413, provide further details on approaches applied, details on antibodies and cytokines used in our experiments, and, in some cases, results for whole-genome sequencing (WGS) and proteomics studies and whole-blood RNA sequencing. The Supplementary Materials and Methods also describes approaches for quantitative real-time RT-PCR (qPCR) and primers used, urate crystal precipitation analyses, and mouse macrophage analyses.

WGS and transcriptome profiling data will be uploaded to NCBI Gene Expression Omnibus database. All patients and healthy volunteers signed a consent form in a protocol approved by each local institutional review board involved in studies on human subjects. All animal procedures were approved by the Chapman University and the San Diego VA Institutional Animal Care and Use Committees. For statistical analyses, *P* values less than 0.05 was considered significant.

RESULTS

Erosive urate crystalline arthritis without hyperuricemia. A 22-year-old White female patient, previously in excellent health and without personal or family history of gout or hyperuricemia, reported sudden-onset nontraumatic left hip pain and presented with antalgic gait. The patient's test for impingement sign was positive, but a plain film radiography of her left hip

San Diego, Collaborative Center of Multiplexed Proteomics. Dr. Terkeltaub's work was supported by VA Research Service grant I01-BX-005927 and NIH grants AR-075990 and PAG-007996. The Genotype-Tissue Expression Project was supported by the Common Fund of the Office of the Director of the NIH and by NCI, NHGRI, NHLBI, NIDA, NIMH, and NINDS.

Drs. Elsaid, Merriman, Rossitto, Liu-Bryan, Karsh, and Phipps-Green contributed equally to this work.

[1]Khaled Elsaid, PharmD, PhD, Sandy Elsayed, MSc: Chapman University School of Pharmacy, Irvine, California; [2]Tony R. Merriman, PhD: Division of Clinical Immunology and Rheumatology, University of Alabama at Birmingham, and Department of Biochemistry, University of Otago, Dunedin, New Zealand; [3]Leigh-Ana Rossitto, BSc, Anaamika Campeau, PhD: Department of Pharmacology, School of Medicine, and Skaggs School of Pharmacy and Pharmaceutical Sciences, UC San Diego, California; [4]Ru Liu-Bryan, PhD: VA San Diego Healthcare System, San Diego, and Department of Medicine, UC San Diego, La Jolla, California; [5]Jacob Karsh, MD, Nancy Maltez, MD: The Ottawa Hospital, Division of Rheumatology, University of Ottawa, Canada; [6]Amanda Phipps-Green, MSc, Murray Cadzow, PhD: Department of Biochemistry, University of Otago, Dunedin, New Zealand; [7]Gregory D. Jay, MD, PhD: Department of Emergency Medicine, Alpert School of Medicine, and Division of Biomedical Engineering, School of Engineering, Brown University, Rhode Island; [8]Marwa Qadri, PharmD, PhD: Jazan University, Jazan, Saudi Arabia; [9]Marin Miner, BSc: VA San Diego Healthcare System, San Diego, California; [10]Talia J. Dambruoso, MSc: Division of Biomedical Engineering, School of Engineering, Brown University, Rhode Island; [11]Tannin A. Schmidt, PhD: Biomedical Engineering Department, School of Dental Medicine, UConn Health, Farmington, Connecticut; [12]Nicola Dalbeth, MD, FRACP, Ashika Chhana, PhD: Department of Medicine, University of Auckland, Auckland, New Zealand; [13]Jennifer Höglund, BSc: Department of Medical Biochemistry, Institute for Biomedicine, University of Gothenburg, Gothenburg, Sweden; [14]Majid Ghassemian, PhD: Biomolecular and Proteomics Mass Spectrometry Facility, Department of Chemistry/Biochemistry, UC San Diego; [15]Niclas G. Karlsson, PhD: Faculty of Health Sciences, Oslo Metropolitan University, Oslo, Norway, and Department of Medical Biochemistry, Institute for Biomedicine, University of Gothenburg, Gothenburg, Sweden; [16]David J. Gonzalez, PhD. Department of Pharmacology, School of Medicine, and Skaggs School of Pharmacy and Pharmaceutical Sciences, Collaborative Center for Multiplexed Proteomics, Program for Integrative Omics and Data Science in Disease Prevention and Therapeutics, UC San Diego, La Jolla, California; [17]Robert Terkeltaub, MD: VA San Diego Healthcare System and Department of Medicine, UC San Diego.

Author disclosures and graphical abstract can be found online at https://onlinelibrary.wiley.com/doi/10.1002/art.42413.

Address correspondence via email to Robert Terkeltaub, MD, at rterkeltaub@health.ucsd.edu.

Submitted for publication July 5, 2022; accepted in revised form November 22, 2022.

was negative for fracture. Tests were negative for presence of rheumatoid factor, anti–cyclic citrullinated peptide antibodies, and antinuclear antibodies. Serum erythrocyte sedimentation rate was increased, and serum C-reactive protein level was elevated. Laboratory test results for renal function were normal. Left hip magnetic resonance imaging showed inflammatory synovitis, joint effusion, and cartilage loss (Figure 1A). Left hip aspiration of synovial fluid yielded negative bacterial cultures; however, synovial fluid contained urate crystals and neutrophils. Serum urate level was normal (5 mg/dl).

Because of progressive left hip pain, the patient required total hip arthroplasty at age 25 years; erosive joint damage and severe cartilage loss were documented on the operative report. In 2012, at age 27 years, the patient was experiencing monthly episodes of self-limiting joint pain and developed swelling, affecting the right wrist, both ankles, and feet. Results of the patient's foot radiographs showed great toe joint erosions with well-defined margins (Figure 1B), consistent with tophaceous, erosive gout. Findings from the patient's ultrasound of the first metatarsophalangeal joint showed subchondral bone erosions and urate crystal deposits (Figure 1C). Ultrasound and dual-energy computed tomography results confirmed urate crystalline macroaggregates in numerous foot joints (Figures 1C–D).

In 2014, after treatment with 400 mg/day allopurinol, serum urate level decreased to ~2 mg/dl and the number of acute arthritis flares markedly lessened. In 2018, the patient underwent genome studies and studies of serum acute-phase reactants and other serum constituents (proteome, lubricin, proteases). In 2019, the patient reported diarrhea episodes, which increased in 2020. Crohn's disease was diagnosed in early 2021 by terminal ileal biopsy findings, which revealed moderate to severe chronic active enteritis, mucosal ulceration, and mucopurulent membranes. She was treated with low-dose budesonide, and her symptoms improved. In 2021, RNA-sequencing studies were performed. None of the research samples were collected at the time of an acute gouty arthritis flare.

Characterization of the proband's inflammatory state. Multiple acute-phase reactants, including C-reactive protein and fibrinogens, were increased in the proband's serum, in serum of the proband's father (who also bore variant NLRP3 V198M), and to a lesser degree in serum of the proband's mother (Figure 2A). Whole-blood RNA-sequencing analyses of globin-depleted RNA and serum proteomics were carried out in proband samples at a time when the symptoms of gout were being controlled over a prolonged period and her symptoms of inflammatory bowel disease had improved. Results of RNA sequencing revealed multiple changes characteristic of an inflammatory disease diathesis phenotype. The proband had 769 differentially expressed genes (DEGs) compared to

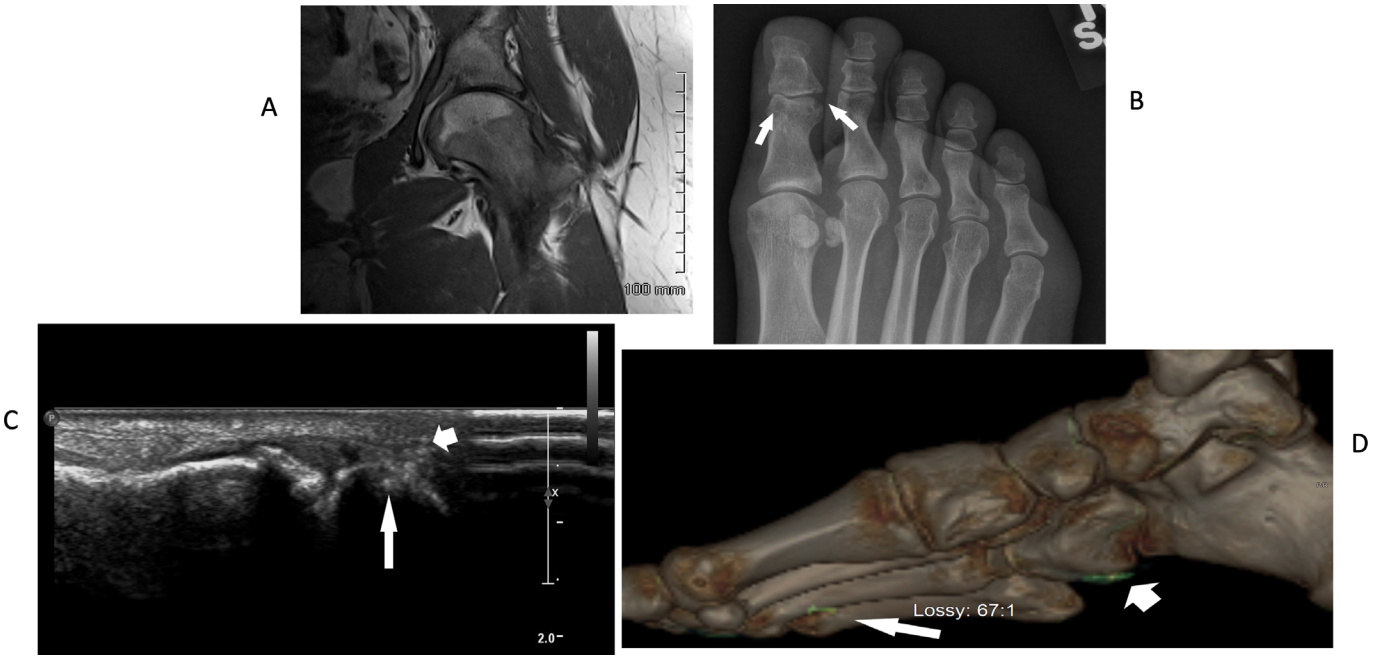

Figure 1. Skeletal imaging in the female proband confirms urate crystal deposition in multiple joints and erosive disease. **A**, Left hip magnetic resonance imaging revealed inflammatory synovitis, joint effusion, and articular cartilage loss. **B**, Foot radiographs revealed classic punched-out great toe joint interphalangeal joint erosions, with well-defined margins (**arrows**), features characteristic of tophaceous, erosive gout. **C**, Ultrasound of first metatarsophalangeal joint revealed hyperechoic areas consistent with urate crystal deposits (**arrowhead**), accompanied by cortical erosion (**arrow**). **D**, Dual-energy computed tomography of the foot confirmed urate crystalline macroaggregates affecting foot joints and surrounding soft tissues (**arrows**). Color figure can be viewed in the online issue, which is available at http://onlinelibrary.wiley.com/doi/10.1002/art.42413/abstract.

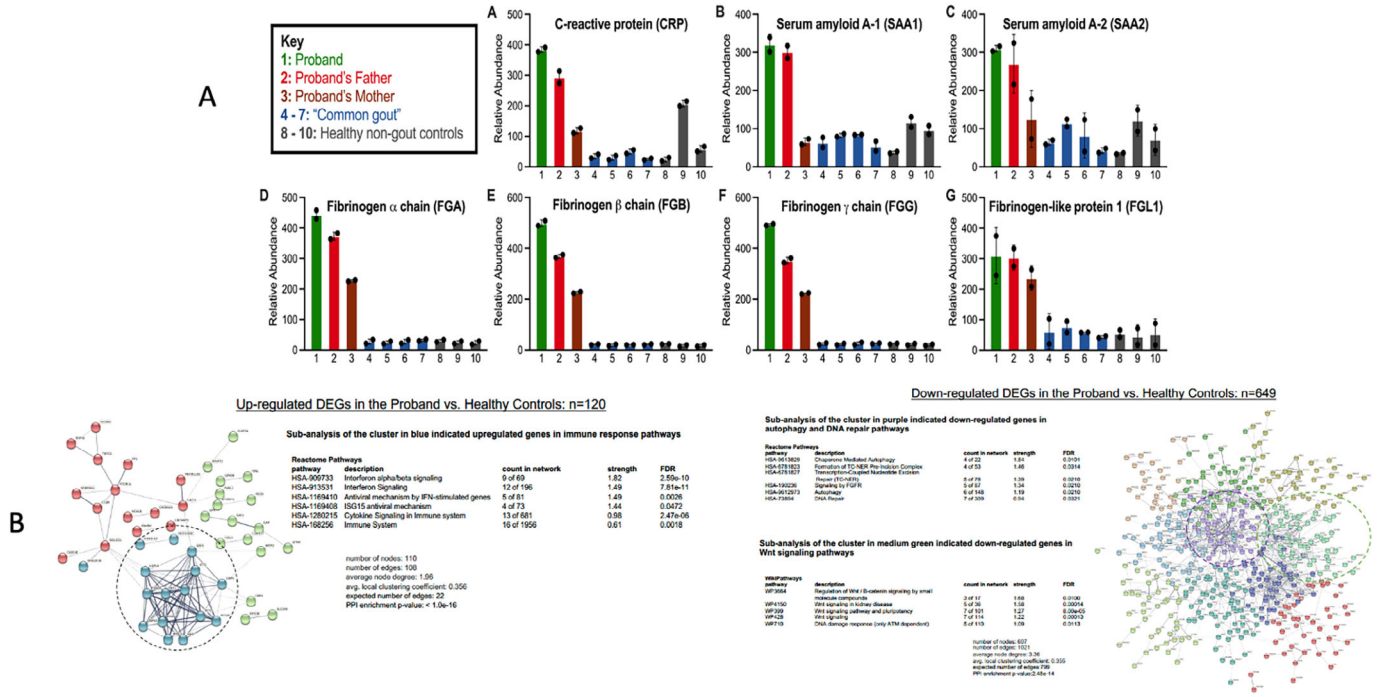

Figure 2. **A**, Relative protein abundances in a panel of acute-phase reactants, measured by quantitative multiplex proteomics, in serum from the female proband, proband's parents, nongout healthy controls (n = 3), and controls with "common gout" but without palpable tolphi (n = 3). Results are the mean and SEM protein relative abundance between replicates (if protein was detected in both replicates). Serum quantitative proteomics showed that multiple acute-phase reactants increased in the female proband, with many also elevated in the proband's father (who also bore the NLRP3 V198M variant) and some increased in the proband's mother. **B**, Key results of whole-blood RNA sequencing in proband compared to 3 nongout healthy controls (using prior depletion of globin RNA, with 2 replicates for each sample). Data analysis shown is further detailed in the Supplementary Materials and Methods, available on the *Arthritis & Rheumatology* website at https://onlinelibrary.wiley.com/doi/10.1002/art.42413. A STRING application protein query generated a node network enriched in differentially expressed genes (DEGs), further separated into 8 clusters. Reactome pathway queries identified functional pathways in each cluster. FDR = false discovery rate; IFN = interferon; ISG15 = interferon-induced 15-kd protein; PPI = protein–protein interaction; FGFR = fibroblast growth factor receptor. Color figure can be viewed in the online issue, which is available at http://onlinelibrary.wiley.com/doi/10.1002/art.42413/abstract.

healthy controls: 120 DEGs were up-regulated, and 649 DEGs were down-regulated. Pathway enrichment analysis of up-regulated genes (Figure 2B) showed a predominance of interferon and cytokine signaling pathways in the proband's whole-blood transcripts compared to blood from healthy controls. Conversely, the RNA-sequencing results showed decreased IL-4 and IL-13 signaling in the proband's serum; IL-4 and IL-13 partially share cell signaling pathways and antiinflammatory and immune-modulating effects. RNA-sequencing results in the proband's whole blood also showed down-regulated chaperone-mediated autophagy and DNA damage and repair response pathways, suggesting impaired cell homeostasis. Further details of the proband's RNA-sequencing analysis are in the Supplementary Materials and Methods and Results and Supplementary Figures b–o, available on the *Arthritis & Rheumatology* website at https://onlinelibrary.wiley.com/doi/10.1002/art.42413.

Lubricin deficiency without decreased whole-blood lubricin messenger RNA (mRNA) expression in the proband. To efficiently screen for erosive gout without hyperuricemia candidate mechanisms, we first examined sera from the proband by label-free proteomics (described in Supplementary Materials and Methods, available at https://onlinelibrary.wiley.com/doi/10.1002/art.42413). Thirteen serum proteins, including lead candidate PRG4/lubricin, were ≥1 order of magnitude decreased in the proband compared to either parent of the proband and to pooled results from 4 healthy controls (Figure 3A). Using multiplex serum quantitative proteomics, with binary comparisons (Figure 3B) (Supplementary Materials and Methods), we classified proteins that were altered "only in proband," "only in family member" (changed versus healthy controls), "only in common gout" (changed in proband and "common gout" patients versus healthy controls), and "nonspecifically" (changed in all binary comparisons). Because significance testing could not be performed for the proband sample analyzed in duplicate, $\log_2$ fold-change cutoff of >0.5 or <0.5 (~40% change) was used to classify proteins as "up-regulated" or "down-regulated," respectively (Supplementary Materials and Methods).

In the proband, 191 proteins were increased or decreased relative to healthy controls, with 119 of these proteins present in the interactome connecting known, physical protein–protein

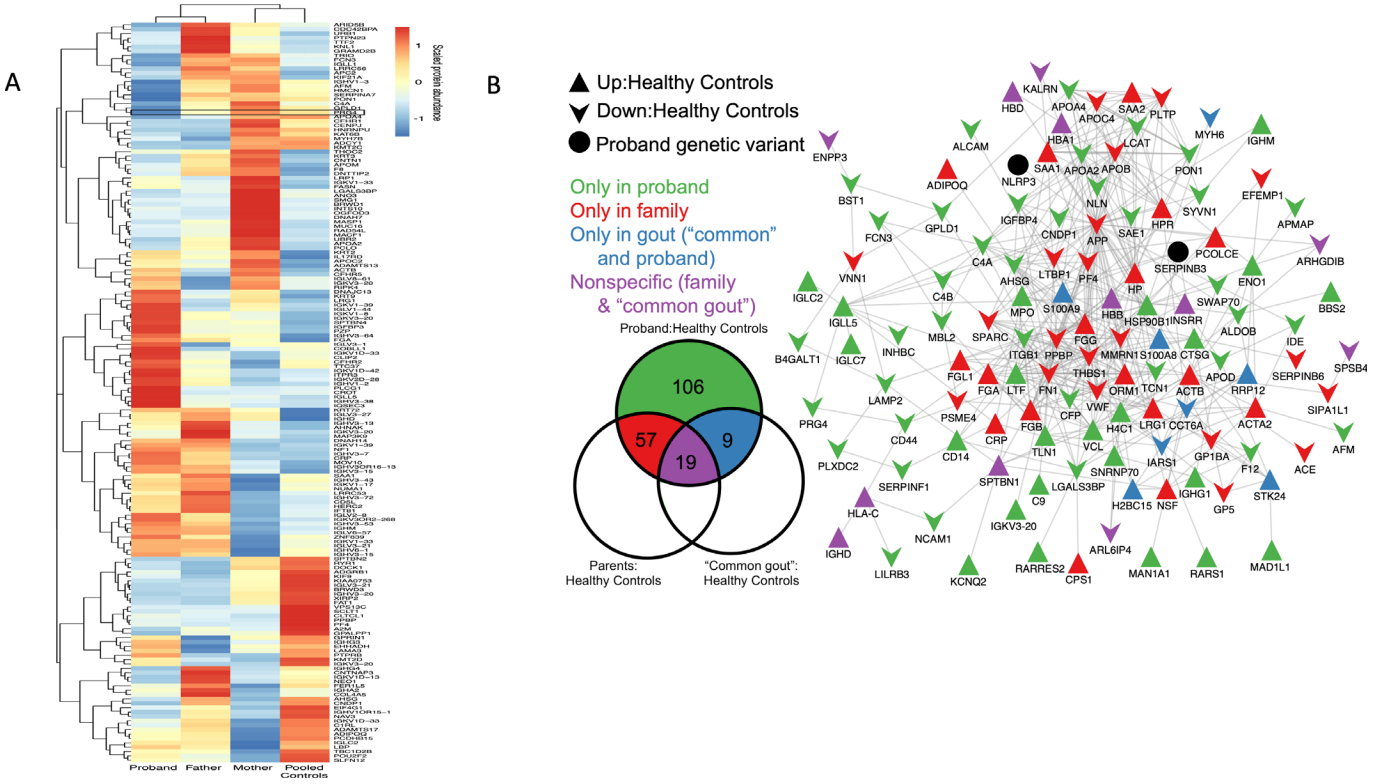

Figure 3. Serum proteomics identifies lubricin attenuation and interactoe network changes in the female proband, suggesting increased lubricin degradation potential. **A**, Label-free proteomics heatmap showing serum proteins, including lead candidate proteoglycan 4 (PRG4)/lubricin, with ~1 order magnitude reduction in the proband versus the father, mother, and pooled (n = 4) nongout healthy controls. **B**, Quantitative multiplex proteomics–defined binary comparisons for proteins with a cutoff of ~40% or more difference between groups. Left, Proteins of interest specific to or overlapping between groups, without directionality (full lists are provided in the Supplementary Proteomics Data Section, available on the *Arthritis & Rheumatology* website at https://onlinelibrary.wiley.com/doi/10.1002/art.42413). Right, Overall proteomics changes in Metascape-generated protein–protein networks, performed using background, edges (known protein–protein interactions), and "pin-dropping" of NLRP3 and SERPINB3 into network. Venn diagram shows network presence of 119 of 191 interacting proteins of interest, suggesting central dysregulated pathways.

interactions (Figure 3B). In sera from the proband and from "common gout" patients, we observed increased levels of the neutrophil-secreted activation biomarkers myeloperoxidase and calprotectin (S100A8, S100A9) (14) (Figure 3B). Significantly, "pin-dropping" NLRP3 and SERPINB3, performed as previously described (15), pointed to NLRP3 and SERPINB3 involvement in the proband interactome.

We analyzed proteins identified in Figure 3B for other altered core pathways, beyond those involving NLRP3 and SERPINB3, that may have promoted the proband's gout phenotype. PRG4/lubricin connected to the soluble form of its receptor CD44 was among the interacting proteins changed in the proband's proteome network. Furthermore, the most centrally connected proteins in the proband's interactome were the cathepsin G (CTSG) substrate (16) amyloid precursor protein, which was relatively low in each kindred member and had 51 network connections, the CTSG inhibitor thrombospondin 1 (TSP-1, THBS1) with 20 connections, lactoferrin (LTF) with 13 connections, and CTSG with 7 connections (Figure 3B). The CTSG inhibitor SERPINB6 was also present in the interactome (17). Results linked lubricin depletion in the proband to potentially enhanced lubricin-degrading capacity.

We confirmed attenuated serum lubricin levels in the proband compared with results shown in serum of the proband's parents and serum of healthy controls (Supplementary Figure 1A, available on the *Arthritis & Rheumatology* website at https://onlinelibrary.wiley.com/doi/10.1002/art.42413) using the dissociation-enhanced lanthanide fluorescent immunoassay, with catching antibody 1E12 (described in Supplementary Materials and Methods, available at https://onlinelibrary.wiley.com/doi/10.1002/art.42413). In immunoassays of lubricin lectin binding, kindred members had slightly elongated O-linked oligosaccharides with increased sialylation in the mucin domain (Supplementary Figure 1A). This suggested disproportionate dominance of more protease-resistant sialic acid–capped lubricin in kindred members' sera.

Competition enzyme-linked immunosorbent assay (ELISA), using lubricin monoclonal antibody 9G3 (18), further validated the findings of markedly low serum lubricin levels in the proband,

which was significantly decreased relative to either parent (neither of them with gout) and to 18 control patients with "common gout" and uncontrolled hyperuricemia at baseline examination before they started the VA STOP GOUT urate-lowering therapy clinical trial (19) (Supplementary Figure 1B). The >30-fold range of serum PRG4/lubricin levels seen in "common gout" patients was far wider than previously seen for patients with rheumatoid arthritis, where serum lubricin levels did not differ significantly from healthy controls (18). Moreover, 5 of the 18 "common gout" subjects had very low levels of serum lubricin.

PRG4 is induced by Wnt signaling in chondrocytes (20). RNA-sequencing pathway enrichment analysis revealed 3 Wnt signaling pathways among those down-regulated in the proband's whole blood relative to healthy controls without gout (Figure 2B). Despite this finding and the finding of blunted serum lubricin levels in the proband, whole-blood *PRG4*/lubricin mRNA was not decreased in the proband compared to either parent or to the healthy controls without gout (Supplementary Figure 1C, available at https://onlinelibrary.wiley.com/doi/10.1002/art.42413).

Imbalance between lubricin-degrading proteases and their inhibitors in the proband. Activity of the lubricin-degrading protease CTSG was increased in sera of the proband, both her parents, and in the "common gout" patients, although with substantial variability. In contrast, CTSG activity was undetectable in unrelated, healthy controls without gout (Figure 4C). ELISA results of "common gout" patient sera also indicated an increased level of the neutrophil-secreted CTSG coactivator LTF compared to matched healthy controls without gout (Figure 4B). Multiplex serum proteomics revealed decreased levels of the normally abundant CTSG and elastase inhibitor TSP-1 (21) and of the predominantly intracellular myeloid leukocyte CTSG inhibitor SERPINB6 in the proband and her parents (17) (Figure 4A). We found no substantial differences between the proband, proband's father and mother, and the nongout and gout control sera for other CTSG inhibitors detected by proteomics, including α_1-antitrypsin (SERPINA1), α_1-antichymotrypsin (SERPINA3), α_1-microglobulin/bikunin precursor, and the inter-α trypsin inhibitor (ITI).

WGS of kindred members. The proband's DNA WGS results (key results summarized in Supplementary Table 1, available on the *Arthritis & Rheumatology* website at https://onlinelibrary.wiley.com/doi/10.1002/art.42413) revealed no obvious functional mutations in *PRG4*. However, the proband and her father shared the *NLRP3* rs121908147 low-penetrance variant that encodes NLRP3 V198M, whose allele frequency is between 0.0038 and 0.0074 in healthy White controls (22,23). NLRP3 V198M, linked to several-fold higher rates of stimulated monocyte IL-1β release in vitro, is occasionally associated with IL-1β–driven autoinflammatory diseases and with periodic fever syndromes (23). The proband was also heterozygous for other potentially disease-promoting *NLRP3* variants (rs4612666, rs10754558, rs4353135, rs6672995) (Supplementary Table 1

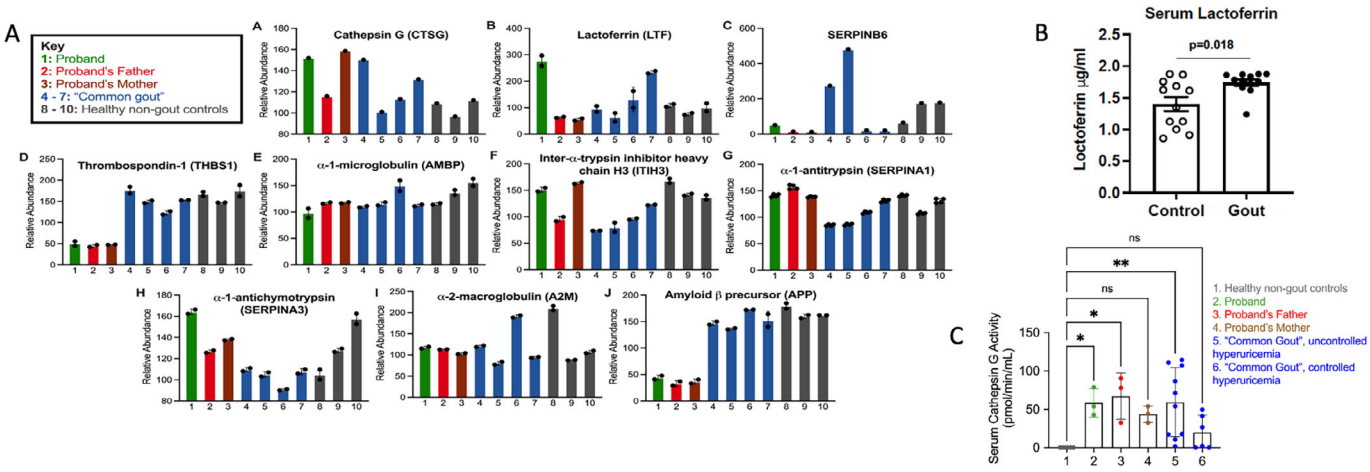

Figure 4. **A,** Serum quantitative multiplex proteomics results for proteins relevant to proteolysis of lubricin in serum from the female proband (patient with gout without hyperuricemia), the proband's father and mother, small pooled samples from "common gout" patients, and nongout healthy controls. Results are the mean and SEM protein relative abundance between replicates (if protein was detected in both replicates). Relevance of individual findings is discussed in the text. **B**, Quantitative results of enzyme-linked immunosorbent assay (ELISA). Serum lactoferrin was increased in "common gout" patients (n = 12) versus nongout healthy controls (n = 12) matched for age, sex, and presence or absence of obesity. Bars show the mean and SEM ELISA results for lactoferrin. **C,** Serum cathepsin G activity (assayed in triplicate) was undetectable in nongout healthy controls (n = 6) but was detected in the female proband, her parents, and multiple patients with gout. "Common gout" patients with hyperuricemia had poorly controlled gout and hyperuricemia at time of sampling (n = 10). "Common gout" patients without hyperuricemia had well-controlled gout (n = 6). In **B** and **C**, symbols represent individual subjects; bars show the mean ± SEM. * = $P < 0.05$; ** = $P < 0.01$, by one-way analysis of variance (ANOVA). ns = not significant. Color figure can be viewed in the online issue, which is available at http://onlinelibrary.wiley.com/doi/10.1002/art.42413/abstract.

and Supplementary Genetics Section B Table 4, available on the *Arthritis & Rheumatology* website at https://onlinelibrary.wiley.com/doi/10.1002/art.42413). To examine the *PRG4* gene further, we extracted all variants in the *PRG4* ± 100-kb regions 1:186165405–186383694. We analyzed 1,318 variants, including those filtered as missense (n = 25), frameshift (n = 5), loss of function (n = 5), and splice (n = 6). No findings of interest were discovered (Supplementary Genetics Section B Tables 2–3).

The proband was heterozygous for the rs74320783 (G523R) variant (Supplementary Genetics Section B Table 5, available on the *Arthritis & Rheumatology* website at https://onlinelibrary.wiley.com/doi/10.1002/art.42413) of ITI heavy chain 3 (*ITIH3*), a multifunctional chondrocyte-expressed Kunitz family inhibitor of multiple serine proteases, including leukocyte elastase and CTSG (24). ITIH3 binds hyaluronan, protects the cartilage surface, and exerts antiinflammatory effects (25). The rs74320783 *ITIH3* variant minor allele frequency is low in European HapMap populations (minor allele frequency = 0.012); in addition, SIFT, PolyPhen, and CADD scores predicted the variant to be deleterious, probably damaging, and likely deleterious, respectively. Moreover, the variant is located at a 11-zinc finger protein or CCCTC-binding factor transcriptional repressor site (CTFC binding site).

The proband was also homozygous for the *SERPINB3* variant rs3180227, which encodes a cysteine protease inhibitory gain-of-function G351V substitution. SERPINB3 is antiapoptotic, proinflammatory, and profibrotic and promotes epithelial to mesenchymal transition (25,26). *SERPINB3* rs3180227 is linked to susceptibility for cirrhosis (27). Deeper analyses of WGS results for selected gene candidates focused on 2 other inhibitors of lubricin-degrading proteases (*SERPINB6*, *THBS1*), which were relatively low in the proband's serum. No obvious variants of interest were identified for *SERPINB6* and *THBS1* (Supplementary Genetics Section B Tables 5–7, available at https://onlinelibrary.wiley.com/doi/10.1002/art.42413). Last, no knockout mutations, or other known rare disease–causing mutations were seen by WGS analysis for any other candidate genes.

Urate blunted crystal formation and suppressed IL-1β–induced xanthine oxidase (XO) activity and uric acid generation by cultured macrophages. IL-1β and tumor necrosis factor (TNF) are known to suppress lubricin mRNA levels in fibroblast-like synoviocytes (FLS) in osteoarthritis, and both IL-1β and TNF promote release of Toll-like receptor 2 (TLR-2) ligands (28,29). Here, we examined additional mechanisms by which deficient intraarticular lubricin release could arise in gouty arthritis. We observed that a TLR-2–selective ligand suppressed PRG4 mRNA and lubricin secretion by human FLS, as did selective activation of TLR-2 in macrophages cocultured in a Transwell system (Supplementary Figure 2, available on the *Arthritis & Rheumatology* website at https://onlinelibrary.wiley.com/doi/10.1002/art.42413). Under the same conditions, the TLR-2 ligand induced human FLS mRNA for cyclooxygenase 2, multiple inflammatory cytokines, and matrix-degrading enzymes.

Articular cartilage homogenates and certain cartilage constituents promote urate crystallization (30,31). In screening tests

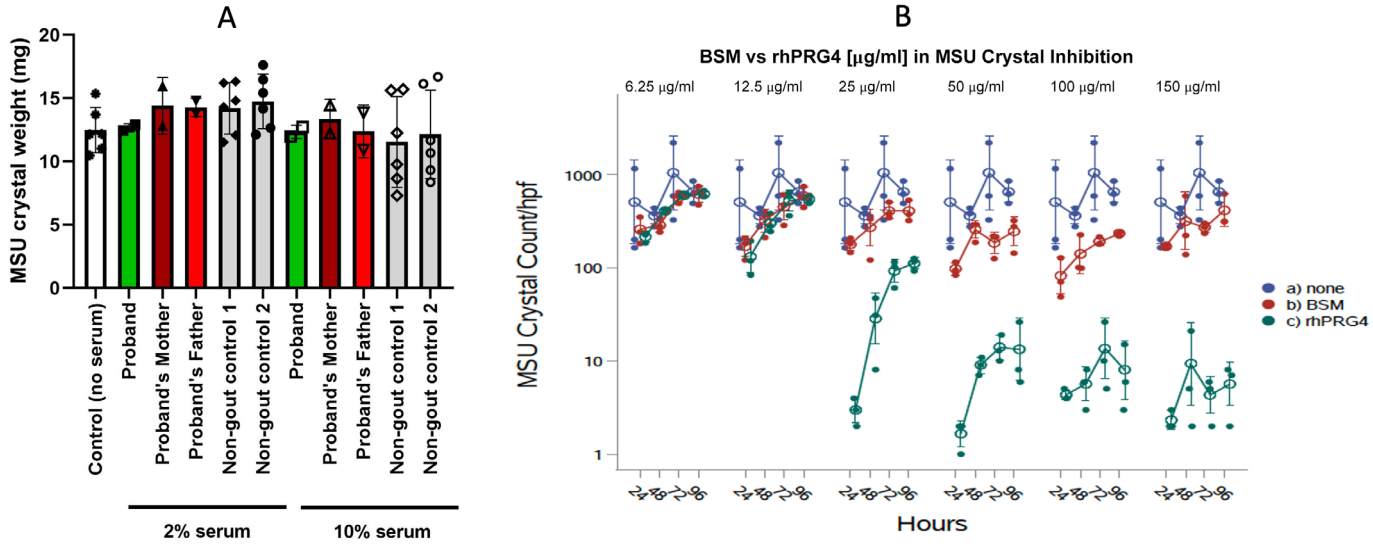

Figure 5. Effects of serum from female proband and of lubricin on monosodium urate (MSU) crystallization. **A**, MSU crystallization over time was assessed using serum urate concentrations of 0.31–0.38 mmoles/liter in either 2% or 10% serum–sodium urate solutions, with serum obtained from the proband, the proband's father and mother, and 2 nongout healthy controls. Results were validated by assessing samples using compensated polarized light microscopy. Symbols represent a single experimental replicate; bars show the mean ± SD. **B**, The number of urate crystals per high-power field (hpf) formed over time was assessed in vitro using cultures of normal serum treated with recombinant human proteoglycan 4 (rhPRG4)/lubricin or bovine submaxillary mucin (BSM) as control, at varying concentrations from 25–150 µg/ml, compared to buffer alone (none) ($P < 0.001$ for rhPRG4/lubricin versus other groups at each dose). Bars show the mean ± SD. Color figure can be viewed in the online issue, which is available at http://onlinelibrary.wiley.com/doi/10.1002/art.42413/abstract.

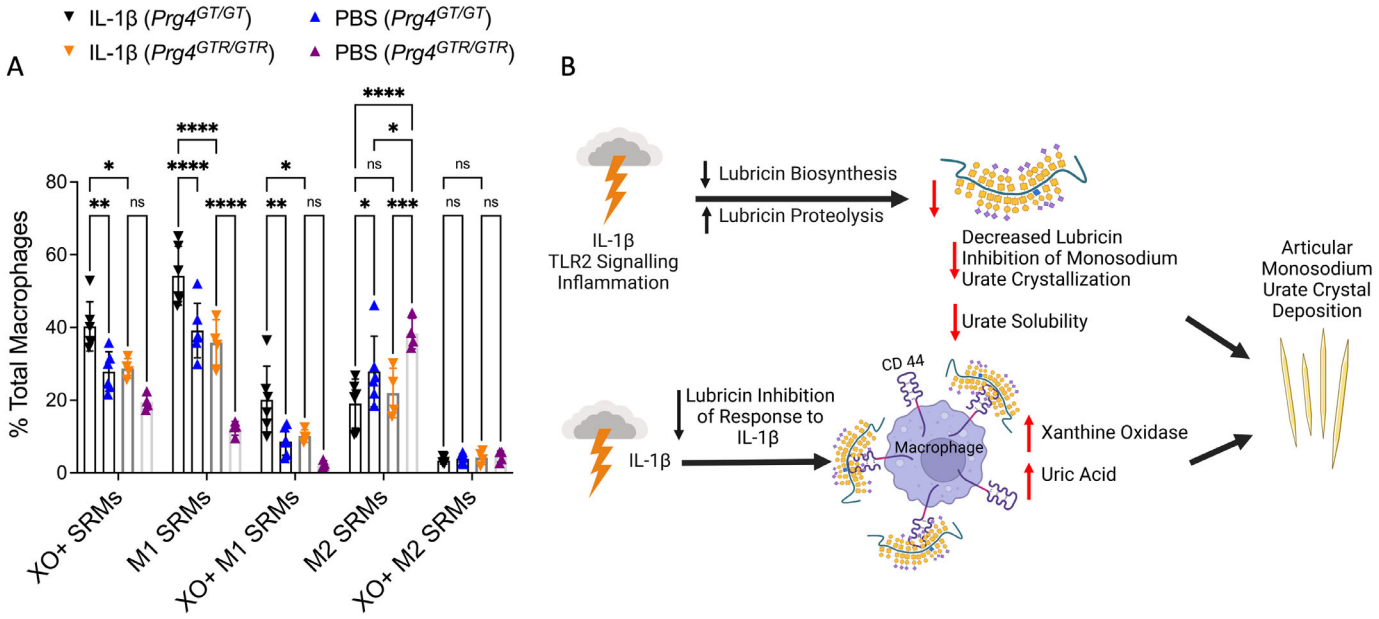

Figure 6. Intraarticular modulation of xanthine oxidase (XO) in synovium-resident macrophages (SRMs), and model for the lubricin and interleukin-1β (IL-1β) circuit regulating gouty arthritis incidence and progression. **A**, Intraarticular IL-1β (10 ng) injection induced XO in SRMs from knees of 2- to 3-month-old Prg4$^{GT/GT}$ mice (n = 6) and Prg4$^{GTR/GTR}$ mice (n = 4). Prg4 reconstitution via recombination of Prg4^{GTR} mice was done, with all mice receiving intraperitoneal tamoxifen at 3 weeks of age. Symbols represent individual mice; bars show the mean ± SD. * = $P < 0.05$; ** = $P < 0.01$; *** = $P < 0.001$; **** = $P < 0.0001$; ns = not significant, by two-way ANOVA with Tukey's pairwise comparisons. **B**, Model for dysfunction of a lubricin and IL-1β regulatory circuit that promotes gout development and progression independent of hyperuricemia, derived from collective results. Color figure can be viewed in the online issue, which is available at http://onlinelibrary.wiley.com/doi/10.1002/art.42413/abstract.

of proband serum, we did not detect any evidence of "hyperprecipitation" of urate crystals in vitro (Figure 5A). Because the lubricin level in normal serum (~1 μg/ml) is much lower than the lubricin level in normal joint fluid (~200 μg/ml) (18), we tested the effects of recombinant human PRG4 on urate crystal formation in vitro (Figure 5B). As a control, we used the large, heavily O-glycosylated molecule bovine submaxillary mucin (BSM), which fails to inhibit urate crystal phagocytosis and cytokine release by macrophages under conditions where lubricin is inhibitory (32). BSM did not significantly affect urate crystallization, whereas lubricin blunted urate crystal formation in vitro (Figure 5B). Lubricin's effect was dose dependent, starting at 25 μg/ml, well below the ~200 μg/ml lubricin concentration shown in normal synovial fluid.

XO promotes macrophage differentiation to an activated state (33). Hence, we tested whether lubricin could limit the potential capacity of macrophage lineage cells within the joint to increase XO activity and generate uric acid in response to IL-1β (Supplementary Figure 3, available on the *Arthritis & Rheumatology* website at https://onlinelibrary.wiley.com/doi/10.1002/art.42413). IL-1β induced increased XO activity and uric acid in wild-type mouse bone marrow macrophages. Because myeloid cells do not make lubricin, we added rhPRG4 to mouse macrophages at 200 μg/ml. Lubricin blunted IL-1β induction of XO and the associated increase in uric acid in cultured bone marrow macrophages.

Last, we assessed synovial resident macrophages (SRMs) that were harvested from mouse knee joint capsules using flow cytometry, conducted as previously reported (34). At baseline, XO positivity was enriched in M1 relative to M2 SRMs in all mouse knee joints studied in vivo (Figure 6A). Baseline XO-positive SRMs were higher in Prg4$^{GT/GT}$ mouse synovia compared to PRG4-reconstituted Prg4$^{GTR/GTR}$ mouse synovia, which was associated with an increase in M1 SRMs. Injection of IL-1β into the mouse knee joint significantly increased XO in total SRMs and in M1 SRMs in Prg4$^{GT/GT}$ versus Prg4$^{GTR/GTR}$ mice. Collective results supported a model (Figure 6B) in which the IL-1β–mediated "inflammatory drive" and phagocyte activation can promote decreased lubricin mRNA in FLS and increased lubricin degradation in the gouty joint. Results suggested that this pathway to lubricin depletion could facilitate IL-1β-induced macrophage XO activity and uric acid generation in the joint and could further lead to intraarticular urate crystal formation in vitro, with these effects occurring independent of hyperuricemia.

DISCUSSION

We characterized a premenopausal female patient (the proband) with normouricemia who had widespread urate crystal deposition, acute inflammatory arthritis flares, destructive unilateral hip arthropathy, great toe erosive joint disease, and classic radiographic features of gout. The collective findings shed new

light on dysregulated articular cell functions, inflammatory responses, and pathways that can impact gout incidence and disease progression independently of hyperuricemia. The proband's arthritis phenotype, compounded later by Crohn's disease, could be classified as an unusual autoinflammatory *NLRP3* variant syndrome, compounded by associated lubricin deficiency and urate crystal deposition that amplified the arthritis. In this context, destructive arthritis first affecting the hip joint is a highly unusual presentation for gout. On the other hand, the proband's arthritis met both sufficient and weighted classification criteria for gout according to the 2015 ACR/EULAR classification criteria (13). The self-limited peripheral arthritis flares and great toe erosions were classic features of gout (1,13). Furthermore, the arthritis markedly responded to long-term allopurinol treatment.

WGS of the proband revealed heterozygosity of *NLRP3* encoding NLRP3 V198M, linked to an increased potential for cryopyrin-associated periodic syndrome and certain other autoinflammatory diseases, and the proband had other potentially deleterious *NLRP3* variants (22,23). Elevated levels of myeloperoxidase, LTF, and calprotectin (S100A8, S100A9) in the proband's serum and in serum samples from gout patients buttressed the evidence of inflammation being linked to heightened neutrophil activation, which can trigger and amplify acute gout (3,35,36). Furthermore, several whole-blood transcript and transcriptional pathway changes in the proband supported the observation of more severe inflammation but also increased macrophage M1 differentiation, which is mediated by XO activity (33). Specifically, IL-4 signaling, which was shown to be decreased in the proband's whole-blood mRNA, promotes macrophage polarization to M2 cells and inhibits macrophage differentiation from M0 to M1 cells. An increase in M2 macrophages is associated with greater release of IL-10 and transforming growth factor β (TGFβ), which may help to self-limit gouty inflammation (35,37). WGS results in the proband also revealed down-regulation in a transcriptional pathway for autophagy, which self-limits gouty inflammation (35), whereas results also revealed an up-regulated cytokine signaling pathway. Hence, the proband appeared predisposed to mount inefficiently resolving inflammatory responses, which were likely contributing to her erosive hip and toe arthritis and later to development of Crohn's disease.

The *PRG4* gene product lubricin was attenuated in proband serum. Lubricin, a large, mucinous boundary lubricant O-glycoprotein, is released in the joint principally by FLS, complemented by chondrocyte release, in the superficial zone, of an alternative *PRG4* gene product, superficial zone protein (SZP) (28,29,38,39). Lubricin regulates synovial macrophage polarization and inflammatory macrophage infiltration (34). Furthermore, *Prg4*-deficient mice demonstrate elevated urate crystal phagocytosis, inflammatory signaling, urate crystal–induced IL-1β release, experimental gout inflammation in vitro and in vivo, and impaired resolution of model acute gouty inflammation (40,41). These effects are mediated by urate crystal binding to the cognate lubricin transmembrane receptor CD44 (42). Because both CD44 knockout and lubricin limit urate crystal–induced inflammation in vivo (40–42), lubricin "cloaking" of CD44 may constitutively suppress synovial proliferation and inflammation in gout.

PRG4 expression is induced by Wnt signaling in chondrocytes (20). In the proband, 3 Wnt signaling transcriptional pathways were decreased. Moreover, both IL-1β and TNF inhibit lubricin mRNA levels in osteoarthritis FLS, and both cytokines promote release of TLR-2 ligands (28,29). In our study, the TLR-2–selective ligand decreased lubricin mRNA and lubricin release in human FLS. In the proband, although whole-blood *PRG4* mRNA was not decreased, lubricin mRNA in the joint space was potentially low.

Joint inflammation promotes lubricin degradation (28,29). The phagocyte-derived protease CTSG cleaves the N-terminal and C-terminal domains in lubricin mucin to generate over 20 lubricin polypeptides (43). Our results supported a pathogenic role in the proband of insufficient inhibition of CTSG and potentially of lubricin-degrading neutrophil elastase. First, an *ITIH3* variant, predicted to be deleterious by 3 different algorithms, was identified in the proband by WGS. The *ITIH3* variant protects articular surfaces from proteolytic damage and acts by binding hyaluronan, inhibiting both CTSG and neutrophil elastase, and limiting complement activation, hyaluronidase activity, and induction of chemokine release (24). Second, the proband, the proband's mother and father, and gout patients tested in our study had increased serum CTSG activity and associated increases in neutrophil-secreted LTF, a co-activator of the abundant, constitutively latent CTSG in azurophil granules. Third, proband serum had decreases in the CTSG inhibitor SERPINB6 and in the tight CTSG and neutrophil elastase inhibitor TSP-1, whose biologic effects include promoting activation from latency of the constitutive gouty inflammation proresolving mediator TGFβ (44).

Results from our study identified novel effects of lubricin on intraarticular urate homeostasis and crystallization. Specifically, lubricin suppressed not only urate crystal deposition in solution but also IL-1β–induced XO activity and urate levels in mouse bone marrow macrophages in vitro and in IL-1β–induced XO in murine SRMs in vivo. FLS lubricin release is significantly inhibited by IL-1β, and this response is limited by lubricin supplementation in vitro (39,45,46). Hence, not only the NLRP3/IL-1β pathway but also modulation of this pathway by lubricin could alter XO activity and urate homeostasis within the joint. Moreover, lubricin decreased urate crystal precipitation in vitro in a dose-dependent manner at 25–150 μg/ml. We tested these lubricin concentrations because synovial fluid lubricin concentration in normal human joints is ~200 μg/ml. Since urate crystallization in vitro is promoted by cartilage homogenates (30,31), these results were unexpected. Notably, failure of the large mucinous O-glycoprotein BSM to suppress urate crystallization in vitro pointed to selectivity of lubricin's effect.

NETosis is a major consequence of neutrophil activation by urate crystals (5), and it is increased in peripheral blood

neutrophils of gout patients (47). NETosis increases tissue urate levels in a DNase-suppressed manner, potentially mediated by extracellular neutrophil DNA accumulation (4), which colocalizes with lubricin-degrading proteases (e.g., neutrophil elastase, CTSG released from granules) and LTF. Since NETosis is linked to formation of tophus-like urate crystal aggregation in experimental gout (47,48), our findings could be mechanistically pertinent to gout.

Serum lubricin is mainly sourced from the liver, and it is not expressed by leukocytes (49). However, lubricin binds several leukocyte adhesion proteins, physiologically coats blood and joint fluid neutrophils, and inhibits both their rolling on endothelium and attachment to articular cartilage (49). As such, elevated phagocyte-derived lubricin–degrading protease activity in serum might be a biomarker for the capacity of phagocytes to degrade lubricin in the joint. Moreover, serum CTSG activity is a potential biomarker in gout, since CTSG promotes inflammation, transduced by effects on matrix metalloproteinase activation, phagocyte movement, and cytokine production under conditions of high neutrophil cell death (50).

Study limitations included that lubricin expression is modulated in a tissue-specific manner; we did not study proband joint tissues or pathology specimens. Directly quantifying the relative effects of G523R substitution in the *ITIH3* variant rs74320783 and deficiencies of TSP-1 and of intracellular SERPINB6 on lubricin-degrading CTSG and elastase activity, as well as studies on NETosis on lubricin homeostasis, were beyond the scope of the work. Because articular chondrocytes express NLRP3, XO, and the *PRG4* gene product SZP, macrophages may not be the sole articular cell type subject to the regulatory effects of NLRP3, IL-1β, and PRG4 on urate homeostasis. We have not detected XO activity in human osteoarthritis FLS (Miner M, Hammaker D, Firestein GS, Terkeltaub R; unpublished observations). However, deeper analyses of articular lubricin and urate homeostasis in cartilage and phagocytes may be of interest. The proband was homozygous for a proinflammatory *SERPINB3* gain-of-function variant, whose net effects in tophus fibrosis, impairment of autophagy, and inflammatory disease in gout remain to be determined. Our proteomics studies used trypsin treatment, which fragments lubricin and other substrates for trypsin and trypsin-like serine proteases. As such, reliably distinguishing between biological proteolysis in serum samples, as opposed to the experimental proteolysis that used trypsin, was not feasible using our proteomics approach. Last, this study combined in vitro bench studies and in vivo mouse studies with proband characterization that included proteomics and transcriptomics. Causal inferences from the bench to the proband were extrapolations that do not conclusively prove the basis for the proband's condition.

In conclusion, lubricin not only suppresses how urate crystals activate macrophages but also inhibits multiple processes central to gout development and progression, such as urate crystal precipitation and IL-1β-induced up-regulation of macrophage XO activity and urate levels. The essential roles of PRG4/lubricin in articular boundary lubrication and joint homeostasis have been illuminated via linkage of severe congenital PRG4/lubricin deficiency to synovial proliferation and joint failure in camptodactyly-arthropathy–coxa vara–pericarditis syndrome (45,46). Lubricin-deficient FLS are more inflammatory, procatabolic, and proliferative (46), and these effects can promote osteoarthritis progression. Hence, articular lubricin dysregulation in osteoarthritis and gout could modulate the frequent coexistence of both diseases. Lubricin homeostasis and its biomarkers, as well as the potential measures to maintain and increase articular lubricin, warrant further investigation for their potential in limiting incidence and progression of gouty arthritis.

ACKNOWLEDGMENTS

Ron Booth and Alicia Storey (The Ottawa Hospital, Ottawa, Canada) were instrumental in organizing study of the proband and the proband's parents in the gout without hyperuricemia kindred. Input on NLRP3 gene variants was provided by Dr. Hal Hoffman (University of California [UC] San Diego). Information on potential lubricin-modulating genes expressed in synovium was shared by Dr. Inka Brockhausen (Queens University, Kingston, Ontario, Canada) and by Drs. Brian Pedersen and Gary Firestein (UC San Diego). Tracy Guo (San Diego VA Healthcare System) provided technical assistance with macrophage and mRNA sample analyses.

The authors acknowledge the use of New Zealand eScience Infrastructure (NeSI) high-performance computing facilities, consulting support, and/or training services as part of this research. New Zealand's national facilities are provided by NeSI and funded jointly by NeSI's collaborator institutions and through the Ministry of Business, Innovation & Employment's research infrastructure program (https://www.nesi.org.nz).

AUTHOR CONTRIBUTIONS

All authors were involved in drafting the article or revising it critically for important intellectual content, and all authors approved the final version to be published. Dr. Terkeltaub had full access to all of the data in the study and takes responsibility for the integrity of the data and the accuracy of the data analysis.

Study conception and design. Elsaid, Merriman, Rossitto, Liu-Bryan, Jay, Karlsson, Gonzalez, Terkeltaub.

Acquisition of data. Elsaid, Merriman, Rossitto, Liu-Bryan, Karsh, Phipps-Green, Jay, Elsayed, Qadri, Miner, Cadzow, Dambruoso, Schmidt, Dalbeth, Chhana, Höglund, Ghassemian, Campeau, Maltez, Karlsson, Gonzalez, Terkeltaub.

Analysis and interpretation of data. Elsaid, Merriman, Rossitto, Liu-Bryan, Karsh, Phipps-Green, Jay, Elsayed, Qadri, Miner, Dalbeth, Karlsson, Gonzalez, Terkeltaub.

REFERENCES

1. Dalbeth N, Merriman TR, Stamp LK. Gout. Lancet 2016;388:2039–52.
2. Chhana A, Dalbeth N. The gouty tophus: a review. Curr Rheumatol Rep 2015;17:19.
3. So A, Dumusc A, Nasi S. The role of IL-1 in gout: from bench to bedside. Rheumatology (Oxford) 2018;57 Suppl:i12–9.

4. Liu C, Zhou M, Jiang W, et al. GPR105-targeted therapy promotes gout resolution as a switch between NETosis and apoptosis of neutrophils. Front Immunol 2022;13:870183.
5. Suzuki K, Tsuchiya M, Yoshida S, et al. Tissue accumulation of neutrophil extracellular traps mediates muscle hyperalgesia in a mouse model. Sci Rep 2022;12:4136.
6. He W, Phipps-Green A, Stamp LK, et al. Population-specific association between ABCG2 variants and tophaceous disease in people with gout. Arthritis Res Ther 2017;19:43.
7. Lu B, Lu Q, Huang B, et al. Risk factors of ultrasound-detected tophi in patients with gout. Clin Rheumatol 2020;39:1953–60.
8. Major TJ, Dalbeth N, Stahl EA, et al. An update on the genetics of hyperuricaemia and gout. Nat Rev Rheumatol 2018;14:341–53.
9. Chen-Xu M, Yokose C, Rai SK, et al. Contemporary prevalence of gout and hyperuricemia in the United States and decadal trends: the National Health and Nutrition Examination Survey, 2007–2016. Arthritis Rheumatol 2019;71:991–9.
10. Vaidya B, Bhochhibhoya M, Nakarmi S. Synovial fluid uric acid level aids diagnosis of gout. Biomed Rep 2018;9:60–4.
11. Towiwat P, Chhana A, Dalbeth N. The anatomical pathology of gout: a systematic literature review. BMC Musculoskelet Disord 2019; 20:140.
12. Tin A, Marten J, Kuhns VL, et al. Target genes, variants, tissues and transcriptional pathways influencing human serum urate levels. Nat Genet 2019;51:1459–74.
13. Neogi T, Jansen TL, Dalbeth N, et al. 2015 Gout classification criteria: an American College of Rheumatology/European League Against Rheumatism collaborative initiative. Arthritis Rheum 2015;67: 2557–68.
14. Shrivastava S, Chelluboina S, Jedge P, et al. Elevated levels of neutrophil activated proteins, α-defensins (DEFA1), calprotectin (S100A8/A9) and myeloperoxidase (MPO) are associated with disease severity in COVID-19 patients. Front Cell Infect Microbiol 2021; 11:751232.
15. Wozniak JM, Mills RH, Olson J, et al. Mortality risk profiling of staphylococcus aureus bacteremia by multi-omic serum analysis reveals early predictive and pathogenic signatures. Cell 2020;182:1311–27.
16. Savage MJ, Iqbal M, Loh T, et al. Cathepsin G: localization in human cerebral cortex and generation of amyloidogenic fragments from the beta-amyloid precursor protein. Neuroscience 1994;60:607–19.
17. Scott FL, Hirst CE, Sun J, et al. The intracellular serpin proteinase inhibitor 6 is expressed in monocytes and granulocytes and is a potent inhibitor of the azurophilic granule protease, cathepsin G. Blood 1999;93:2089–97.
18. Ai M, Cui Y, Sy MS, et al. Anti-lubricin monoclonal antibodies created using lubricin-knockout mice immunodetect lubricin in several species and in patients with healthy and diseased joints. PLoS One 2015;10: e0116237.
19. O'Dell JR, Brophy MT, Pillinger MH, et al. Comparative effectiveness of allopurinol and febuxostat in gout management. NEJM Evid 2022; 1:10.1056/evidoa2100028.
20. Xuan F, Yano F, Mori D, et al. Wnt/β-catenin signaling contributes to articular cartilage homeostasis through lubricin induction in the superficial zone. Arthritis Res Ther. 2019;21:247.
21. Hogg PJ, Owensby DA, Chesterman CN. Thrombospondin 1 is a tight-binding competitive inhibitor of neutrophil cathepsin G. Determination of the kinetic mechanism of inhibition and localization of cathepsin G binding to the thrombospondin 1 type 3 repeats. J Biol Chem 1993; 268:21811–8.
22. Rowczenio DM, Trojer H, Russell T, et al Clinical characteristics in subjects with NLRP3 V198M diagnosed at a single UK center and a review of the literature. Arthritis Res Ther 2013;15:R30.
23. Kuemmerle-Deschner JB, Verma D, Endres T, et al. Clinical and molecular phenotypes of low-penetrance variants of NLRP3: diagnostic and therapeutic challenges. Arthritis Rheumatol 2017;69: 2233–40.
24. Lord MS, Melrose J, Day AJ, et al. The anter-α-trypsin inhibitor family: versatile molecules in biology and pathology. J Histochem Cytochem 2020;68:907–27.
25. Turato C, Biasiolo A, Pengo P, et al. Increased antiprotease activity of the SERPINB3 polymorphic variant SCCA-PD. Exp Biol Med (Maywood) 2011;236:281–90.
26. Sivaprasad U, Kinker KG, Ericksen MB, et al. SERPINB3/B4 contributes to early inflammation and barrier dysfunction in an experimental murine model of atopic dermatitis. J Invest Dermatol 2015;135: 160–9.
27. Turato C, Ruvoletto MG, Biasiolo A, et al. Squamous cell carcinoma antigen-1 (SERPINB3) polymorphism in chronic liver disease. Dig Liver Dis 2009;41:212–6.
28. Elsaid KA, Jay GD, Chichester CO. Reduced expression and proteolytic susceptibility of lubricin/superficial zone protein may explain early elevation in the coefficient of friction in the joints of rats with antigen-induced arthritis. Arthritis Rheum 2007;56:108–16.
29. Svala E, Jin C, Rüetschi U, et al. Characterisation of lubricin in synovial fluid from horses with osteoarthritis. Equine Vet J 2017;49:116–23.
30. Chhana A, Pool B, Wei Y, et al. Human cartilage homogenates influence the crystallization of monosodium urate and inflammatory response to monosodium urate crystals: a potential link between osteoarthritis and gout. Arthritis Rheumatol 2019;71:2090–9.
31. Chhana A, Lee G, Dalbeth N. Factors influencing the crystallization of monosodium urate: a systematic literature review. BMC Musculoskelet Disord 2015;16:296.
32. Qadri M, Jay GD, Zhang LX, et al. Recombinant human proteoglycan-4 reduces phagocytosis of urate crystals and downstream nuclear factor κ B and inflammasome activation and production of cytokines and chemokines in human and murine macrophages. Arthritis Res Ther 2018;20:192.
33. Gibbings S, Elkins ND, Fitzgerald H, et al. Xanthine oxidoreductase promotes the inflammatory state of mononuclear phagocytes through effects on chemokine expression, peroxisome proliferator-activated receptor-{γ} sumoylation, and HIF-1a. J Biol Chem 2011;286: 961–75.
34. Qadri M, Jay GD, Zhang LX, et al. Proteoglycan-4 is an essential regulator of synovial macrophage polarization and inflammatory macrophage joint infiltration. Arthritis Res Ther 2021;23:241.
35. Terkeltaub R. What makes gouty inflammation so variable? BMC Med 2017;15:158.
36. Johnson JL, Ramadass M, Haimovich A, et al. Increased neutrophil secretion induced by NLRP3 mutation links the inflammasome to azurophilic granule exocytosis. Front Cell Infect Microbiol 2017;7:507.
37. Chen YH, Hsieh SC, Chen WY, et al. Spontaneous resolution of acute gouty arthritis is associated with rapid induction of the anti-inflammatory factors TGFβ1, IL-10 and soluble TNF receptors and the intracellular cytokine negative regulators CIS and SOCS3. Ann Rheum Dis 2011;70:1655–63.
38. Rhee DK, Marcelino J, Baker M, et al. The secreted glycoprotein lubricin protects cartilage surfaces and inhibits synovial cell overgrowth. J Clin Invest 2005;115:622–31.
39. Alquraini A, Jamal M, Zhang L, et al. The autocrine role of proteoglycan-4 (PRG4) in modulating osteoarthritic synoviocyte proliferation and expression of matrix degrading enzymes. Arthritis Res Ther 2017;19:89.
40. Qadri M, Jay GD, Zhang LX, et al. Recombinant human proteoglycan-4 reduces phagocytosis of urate crystals and downstream nuclear factor γ B and inflammasome activation and

production of cytokines and chemokines in human and murine macrophages. Arthritis Res Ther 2018;20:192.

41. El Sayed S, Jay GD, Cabezas R, et al. Recombinant human proteoglycan 4 regulates phagocytic activation of monocytes and reduces IL-1β secretion by urate crystal stimulated gout PBMCs. Front Immunol 2021;12:771677.
42. Bousoik E, Qadri M, Elsaid KA. CD44 receptor mediates urate crystal phagocytosis by macrophages and regulates inflammation in a murine peritoneal model of acute gout. Sci Rep 2020;10:5748.
43. Huang S, Thomsson KA, Jin C, et al. Cathepsin g degrades both glycosylated and unglycosylated regions of lubricin, a synovial mucin. Sci Rep 2020;10:4215.
44. Murphy-Ullrich JE, Suto MJ. Thrombospondin-1 regulation of latent TGF-β activation: a therapeutic target for fibrotic disease. Matrix Biol 2018;68-69:28–43.
45. Jones AR, Flannery CR. Bioregulation of lubricin expression by growth factors and cytokines. Eur Cell Mater 2007;13:40–5.
46. Alquraini A, Jamal M, Zhang L, et al. The autocrine role of proteoglycan-4 (PRG4) in modulating osteoarthritic synoviocyte proliferation and expression of matrix degrading enzymes. Arthritis Res Ther 2017;19:89.
47. Vedder D, Gerritsen M, Nurmohamed MT, et al. A neutrophil signature is strongly associated with increased cardiovascular risk in gout. Rheumatology (Oxford). 2021;60:2783–90.
48. Schauer C, Janko C, Munoz LE, et al Aggregated neutrophil extracellular traps limit inflammation by degrading cytokines and chemokines. Nat Med 2014;20:511–7.
49. Jin C, Ekwall AK, Bylund J, et al. Human synovial lubricin expresses sialyl Lewis x determinant and has L-selectin ligand activity. J Biol Chem. 2012;287:35922–33.
50. Gao S, Zhu H, Zuo X, et al. Cathepsin G and its role in inflammation and autoimmune diseases. Arch Rheumatol 2018;33: 498–504.